Natural Gas Hydrate Formation and Decomposition in the Presence of Kinetic Inhibitors. 3. Structural and Compositional Changes

ARTICLE *in* ENERGY & FUELS · SEPTEMBER 2011

Impact Factor: 2.79 · DOI: 10.1021/ef200814z

4 AUTHORS:

N. Daraboina
University of Tulsa
36 PUBLICATIONS **406** CITATIONS
SEE PROFILE

John A. Ripmeester
National Research Council Canada
714 PUBLICATIONS **15,661** CITATIONS
SEE PROFILE

Virginia Walker
Queen's University
168 PUBLICATIONS **4,045** CITATIONS
SEE PROFILE

Peter Englezos
University of British Columbia - Vancouver
171 PUBLICATIONS **4,787** CITATIONS
SEE PROFILE

energy&fuels

ARTICLE

pubs.acs.org/EF

Natural Gas Hydrate Formation and Decomposition in the Presence of Kinetic Inhibitors. 3. Structural and Compositional Changes

Nagu Daraboina,[†] John Ripmeester,[‡] Virginia K. Walker,[§] and Peter Englezos*[,†]

[†]Department of Chemical and Biological Engineering, University of British Columbia Vancouver, British Columbia, Canada

[‡]Steacie Institute for Molecular Sciences, National Research Council Canada, Ottawa, Ontario, Canada

[§]Department of Biology, Queen's University, Kingston, Ontario, Canada

ABSTRACT: A synthetic natural gas mixture composed of methane, ethane, and propane in a batch reactor was used to form gas hydrates in the presence of two commercial, chemical kinetic inhibitors, polyvinylpyrrolidone (PVP) and H1W85281, and one biological inhibitor, antifreeze protein type III (AFP-III). Powder X-ray diffraction and nuclear magnetic resonance spectroscopy showed that structure II hydrates dominated, as expected, but in the presence of the chemical inhibitors, structure I was also present. Raman spectroscopy confirmed the complexity and the heterogeneity of the guest composition within these hydrates, which was also consistent with the gas analysis obtained using gas chromatography. However, in the presence of AFP-III, hydrates appeared to be relatively homogeneous structure II hydrates, with weaker evidence of structure I. When individual gas cage occupancies were calculated, both classes of inhibitors reduced large cage methane occupancy by ~25%. With the chemical inhibitors, these large cage methane guests appeared to be substituted by ethane, likely resulting in a decreased driving force for hydrate production. In contrast to the near full occupancy of large cages with these inhibitors, almost 10% of the large cages were not filled when hydrates were formed in the presence of AFP-III, likely contributing to the easy decomposition of such hydrates seen in other studies. Therefore, hydrates formed in the presence of these two classes of inhibitors appear to be distinct, and as a consequence, their inhibition mechanisms, as well their practical utility in the field, are likely to be marked by important differences.

I. INTRODUCTION

Natural gas hydrates are crystalline compounds composed of hydrocarbon guest molecules enclathrated in a water molecule framework that form under suitable temperature and pressure conditions. Three known hydrate structures exist, distinguished by the size and geometry of the water framework: Structure I (sI) generally enclathrates small hydrocarbons such as methane or ethane, with structure II (sII) housing larger molecules such as propane.[1,2] These two structures are cubic, but the third type, structure H (sH), has a hexagonal crystal structure, which can enclathrate molecules as large as methylcyclopentane or two guest molecules such as methane and dimethylbutane.[3] It has only rarely been reported in nature,[4] as it appears to be present as a minor component and its identification is not trivial. In addition to these restrictions, when a gas mixture is present, the formed hydrates may be more complex than those with a single component. For example, a mixture of methane and ethane can form sI if the methane concentration is below 75% or above 99% but can form sII at intermediate compositions.[5,6] Uchida et al.[7] reported that mixed methane and propane gases form sI and sII in two steps, with propane favored for enclathration, resulting in an enriched methane gas phase or a fractionation effect. In natural gas mixtures with three components, methane, ethane, and propane, both sI and sII hydrates can form simultaneously depending on the gas composition.[8] Although the structures, cage occupancies, and compositions of mixed gas hydrates have been reported,[7,9−12] the hydrate preparation protocol may impact these,[13,14] strongly suggesting that kinetics can play a significant role. Although the complexity associated with natural gas hydrates is daunting, it is nevertheless crucial information for industry in their efforts to manage hydrate formation.

Because gas hydrates can impede the flow and cause blockage in pipelines and because there are safety and economic concerns associated with the use of thermodynamic inhibitors, the oil and gas industry has shifted their attention toward kinetic hydrate inhibitors (KHIs) to delay or prevent hydrate formation.[15] Some of these, such as polyvinylpyrrolidone (PVP), have been studied for several years,[15,16] and others, such as the new propriety inhibitor H1W85281, have been developed more recently. Biologically based antifreeze proteins (AFPs) have also shown efficacy in hydrate inhibition under laboratory conditions.[17−19] However, it is significant that, despite two decades of effort, the inhibiting action of neither the synthetic chemicals nor the proteins is understood,[15,20] even with single gas hydrate formers.

Despite the challenge, there can be little doubt that understanding the enclathration of natural gas mixtures in the presence of KHIs would greatly assist in the development of future inhibitors to manage hydrate formation in the field. Traditionally, powder X-ray diffraction (PXRD) has been used to determine the type of hydrate,[7,12,14] with Raman spectroscopy used as a tool for guest identification and, in certain circumstances, hydrate composition and cage occupancy.[11,12,21,22] A third technique, ^{13}C NMR spectroscopy, has also proved useful for obtaining quantifiable cage occupancies of mixed gas hydrate.[9,10,12,23,24]

Received: June 1, 2011
Revised: August 13, 2011
Published: August 13, 2011

Table 1. Vapor Phase Composition during Hydrate Formation in the Absence (Water) or the Presence of Various Inhibitors at 9.0 MPa and 274 K

	water			PVP			H1W85281			AFP		
time (min)	CH_4	C_2H_6	C_3H_8	CH_4	C_2H_6	C_3H_8	CH_4	C_2H_6	C_3H_8	CH_4	C_2H_6	C_3H_8
0	0.930	0.050	0.020	0.930	0.050	0.020	0.930	0.050	0.020	0.930	0.050	0.020
15	0.932	0.047	0.021	0.933	0.049	0.018	0.932	0.049	0.019	0.931	0.048	0.021
30	0.933	0.048	0.019	0.936	0.047	0.017	0.937	0.047	0.016	0.934	0.046	0.020
45	0.938	0.048	0.014	0.941	0.045	0.014	0.944	0.044	0.012	0.937	0.044	0.019
60	0.94	0.047	0.013	0.944	0.042	0.014	0.949	0.04	0.011	0.942	0.045	0.013
90	0.943	0.044	0.013	0.948	0.039	0.013	0.953	0.037	0.01	0.945	0.041	0.014
120	0.944	0.042	0.014	0.952	0.036	0.012	0.956	0.034	0.01	0.947	0.039	0.014
150	0.945	0.041	0.014	0.956	0.033	0.011	0.961	0.030	0.009	0.948	0.037	0.015

As indicated, only a few molecular descriptions are available for natural gas hydrates in the presence of inhibitors,[13,15,16,25,26] but they suggest that inhibitors can have an impact on the structure and composition of mixed hydrates. Exothermic and endothermic peak analyses reflecting hydrate formation and disassociation, respectively, and monitored by differential scanning calorimetry (DSC) were more complex in the presence of two chemical KHIs: PVP and H1W85281.[27] In addition, hydrates formed in a stirred reactor with these KHIs decomposed in two stages, again suggestive of mixed structures.[28] Here, we observed the effect of chemical and biological KHIs on natural gas hydrate formation using three solid state analytical techniques, in addition to gas chromatography, to measure the vapor phase composition changes during hydrate formation. It is our belief that knowledge of the guest distribution and homogeneity of the hydrate products is important for an understanding of the inhibition mechanisms of different KHIs.

II. EXPERIMENTAL SECTION

A. Materials. Two commercial, chemical hydrate kinetic inhibitors polyvinylpyrrolidone (PVP; ~10 kDa, from Sigma Aldrich) and H1W85281 (~3 kDa, a proprietary commercial product of unknown composition) were used. The active ingredient concentration of the H1W85281 was 40 wt %. The biological inhibitor type III AFP (~7 kDa, purchased from A/F Protein Canada Inc., Swiss Prot Database accession number P19414) was obtained by fermentation and secretion from recombinant *Saccharomyces cerevisiae* yeast cells, purified by differential diafiltration and kept at −20 °C until used. Deionized water was used to dilute the inhibitors to 0.1 mM. A synthetic natural gas mixture consisting of methane (93%)/ethane (5%)/propane (2%) was used in all experiments. It was at extra high purity and purchased from Praxair Canada.

1. Sample Preparation. To prepare hydrate samples, water (3 mL) and inhibitor (0.1 mM PVP, H1W85281, or AFP-III) solutions were frozen (253 K), ground, and then loaded into a 50 mL pressure vessel. The loading was performed in the freezer (~253 K) to prevent the melting of ice. The vessel was pressurized with the methane/ethane/propane mixture until 9 MPa and kept in the cooler for about 1 h until the solutions nucleated. The vessel was then transferred to a water bath maintained at 274 K. After 48 h, the hydrate samples were collected from the vessel under liquid nitrogen and stored in liquid nitrogen to avoid hydrate decomposition.

2. Gas Phase Analysis. A Varian CP-3800 gas chromatograph (GC) with a thermal conductivity detector, flame ionization detector, and CP-PoraPLOT U capillary column was used to analyze the hydrate samples. Ultrahigh purity He was used as the carrier gas. The gas sample was transferred from the crystallizer to a 3.1 mm stainless steel sampling tube, with a volume of 300 μL. Considering that the volume of the crystallizer is 323 mL, sampling did not affect the mass balance calculations.[29] The sampling tube was flushed three times with He before samples were collected for analysis. Subsequently, the gas from the sampling tube was injected into the GC through a six-port valve with a sampling loop (100 μL).

3. Powder X-ray Diffraction. To obtain crystal structure information on hydrates, PXRD measurements were obtained on an instrument (40 kV, 40 mA, BRUKER axs model D8 advance) using a $\theta/2\theta$ step scan mode, a step size of 0.01, and a counting time of 0.4 s/step using Cu Kα radiation (λ = 1.5406). The measurements were performed at atmospheric pressure and 125 K to prevent hydrate dissociation.

4. Raman Spectroscopy. Hydrate samples were further analyzed with an Acton Raman spectrograph equipped with fiber optics, a grating (1200 grooves/mm), and a charged couple detector (CCD). An Ar-ion laser was used as the excitation source (514.53 nm). The laser was focused on the sample using a 10× microscope objective. The spectrograph was computer-controlled, and spectra were recorded with a 1 s integration time over 200 scans.

5. NMR Spectroscopy. A DSX 400 MHz NMR spectrometer was used to record ^{13}C spectra for the hydrate samples. Guest ^{13}C resonance intensities were used to determine the cage occupancy of individual gases and the gas composition of the hydrate samples. A zirconium rotor charged with powdered hydrate at low temperatures was loaded into a low temperature probe maintained at 173 K. Single pulse excitation (90° of 5 μs) and pulse repetition delay of 300 s under proton decoupling and magic angle spinning at 2.5 kHz were employed to record spectra. The detailed procedure has been described in ref 12. The cage occupancies were calculated using the assumptions and descriptions provided in methods in refs 9, 10, 12, and 24.

III. RESULTS AND DISCUSSION

A. Gas Phase Analysis and Powder XRD. When hydrates were formed from the mixed gases, gas phase analysis showed that the concentration of methane increased from 93 to 94.5% over 2.5 h (Table 1). The increase was mirrored with a gas phase decrease in the ethane and propane concentrations from 5 to 4.1% and from 2 to 1.4%, respectively. This is evidence of the fractionation that takes place during gas hydrate formation with pure water[29,30] and is likely due to different rates of incorporation of the three gas components in the hydrate lattice.

The addition of chemical KHIs (PVP and H1W85281) changed the proportion of the gases in the vapor phase. In the presence of PVP, the concentration of methane was 1% higher than that in water controls after 2.5 h, and it reached 95.6% after

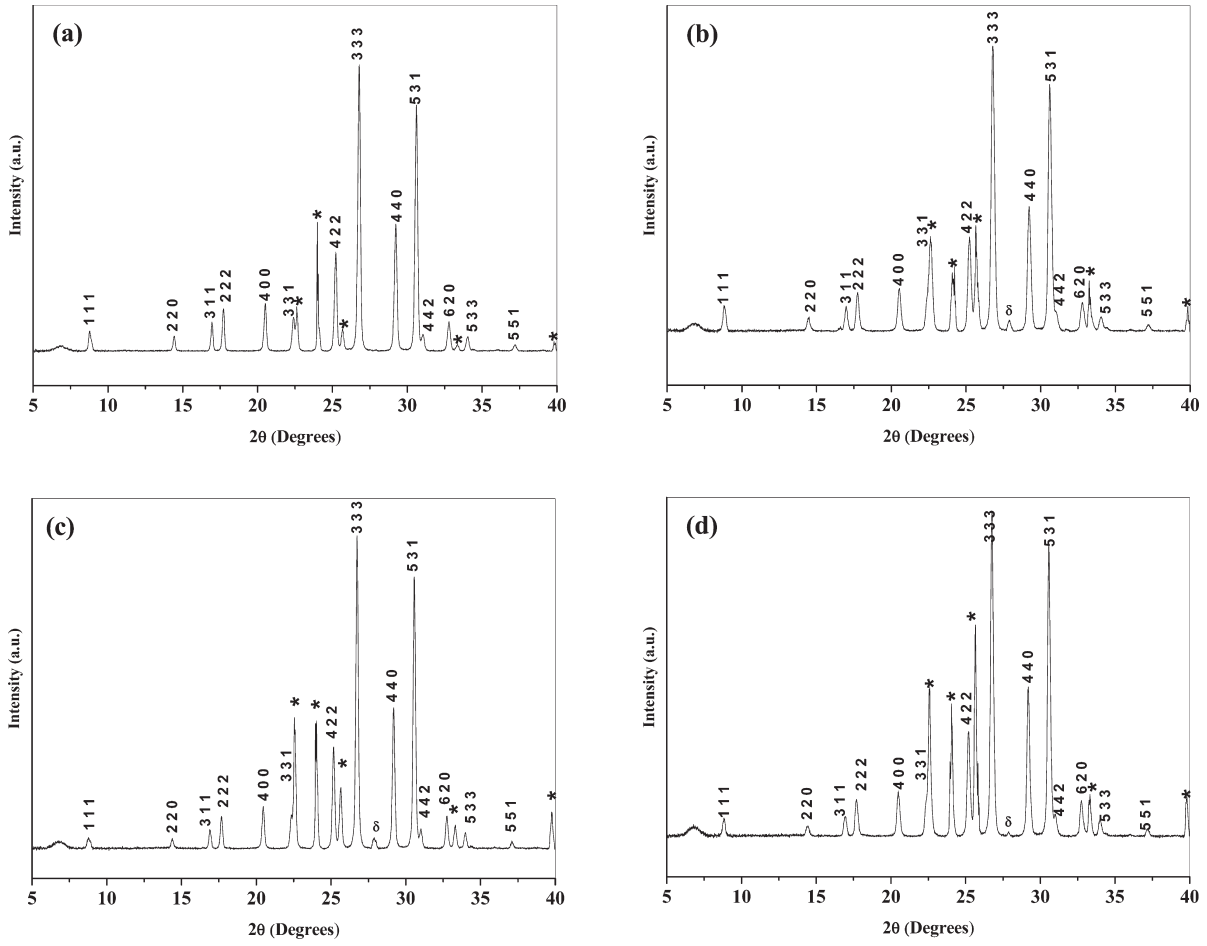

Figure 1. PXRD pattern obtained at 125 K for a hydrate sample synthesized from a methane/ethane/propane/water mixture at 9.0 MPa and 274 K (the sI peak is indicated by δ; ice peaks are indicated by *): (a) control experiments with no additives, (b) PVP, (c) H1W85281, and (d) AFP-III.

2.5 h (Table 1). Similarly, compared to the controls, concentrations of ethane and propane decreased and reached 3.3 and 1.1%, respectively. Likewise, in the presence of H1W85281, the concentration of methane after 2.5 h was 96.1% and those of ethane and propane decreased to 3.0 and 0.9%, respectively. The biological inhibitor AFP-III did have some influence on the gas phase, but it was not as notable as that of the commercial KHIs. The concentration of methane in the gas phase reached 94.8%, and those of ethane and propane decreased to 3.7 and 1.5%, respectively. From these results, it is evident that, at least in the presence of the chemical inhibitors and perhaps with AFP-III, there is an impact on gas consumption, with the heavier hydrocarbons (ethane and propane) appearing to preferentially incorporate into hydrates during the early stages.

Because gas phase analysis indicated that the different classes of KHIs could have an impact on guest gas incorporation, PXRD was used to determine the type of hydrate formed. When hydrates were prepared at 274 K and 9 MPa without any inhibitors, sII hydrates were present (Figure 1a), as expected.[2] PXRD patterns also showed that although sII hydrates were predominantly formed in the presence of the KHIs, some sI was also detected (Figure 1; indicated by the peaks marked with a δ). The sI peak was most obvious in hydrates formed with PVP and H1W85281 (Figure 1b and c) and was so small that it was difficult to detect in the AFP-containing samples (Figure 1d). This result confirms our previous suspicions based on DSC analysis[27] and stirred tank experiments[28] that more complex hydrates are formed in the presence of chemical inhibitors. The PXRD patterns also revealed the presence of ice (Figure 1; indicated by peaks marked with *). Because the ice peak intensities were higher in the presence of all of the tested KHIs compared to controls prepared without inhibitors, it is apparent that the conversion of ice to hydrate was impeded with the additives, which has never been reported previously with PXRD. A slower ice to hydrate conversion is consistent with the inhibition activities of KHIs.

B. Raman Spectroscopy. Once the presence of hydrate was confirmed in the solid phase, the samples were analyzed using Raman and NMR spectroscopy to obtain cage occupancies, hydration numbers, and localized as well as overall hydrate composition. Raman spectra obtained from hydrates formed without inhibitors clearly showed the C−H region from 2800 to 3000 cm^{-1} and the O−H region from 3000 to 3400 cm^{-1} (Figure 2a). Two peaks at ~2904 and 2914 cm^{-1} represented the C−H stretch vibration from methane molecules encaged in large and small cages, respectively. Other small peaks in the C−H region were derived from ethane and propane in the large cages. Peak positions around 2870, 2878, and 2984 cm^{-1} represented C−H stretching vibrations of propane in large cages, with peak positions at 2884 and 2940 cm^{-1} corresponding to ethane. The broad peak at 3090 cm^{-1} represents the vibrational mode of water molecules in the host lattice of the hydrate structure.[12,21,31]

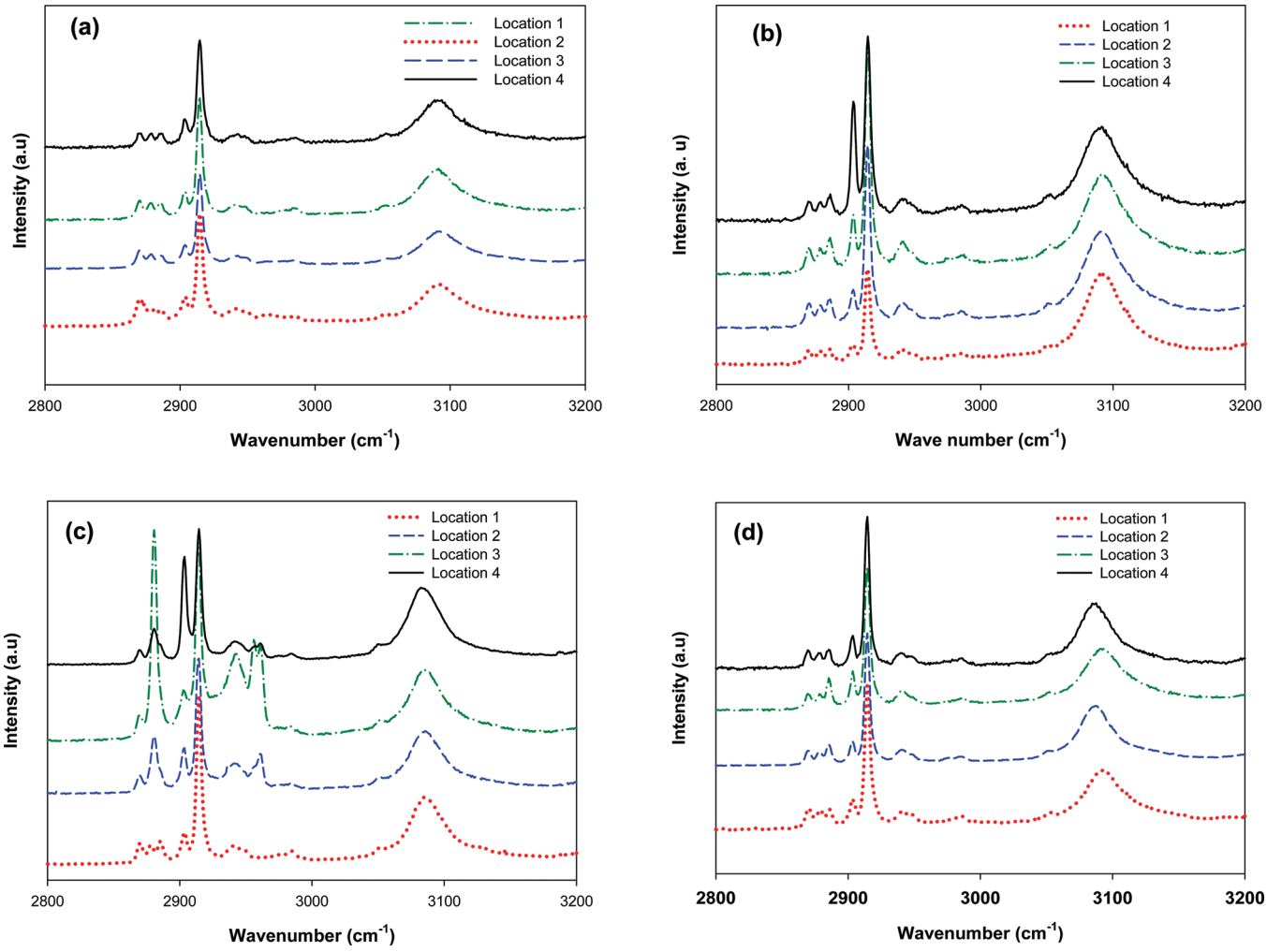

Figure 2. Raman spectra of methane/ethane/propane hydrate formed with (a) no additives (control experiments), (b) PVP, (c) H1W85281, and (d) AFP-III.

When spectra were obtained for four different locations in the same sample, no significant differences were observed, demonstrating consistency in the spectra obtained in the water controls (Figure 2a).

Contrary to the consistent spectra obtained without inhibitors, the presence of chemical KHIs resulted in substantially different profiles even though they were obtained from the same samples (Figure 2b and c). For example, the peak at 2904 cm^{-1} for methane in large cages varied considerably in the profiles for PVP (Figure 2b). Although it is difficult to distinguish between peaks for sI and sII in the C−H stretch region because of strongly overlapping peaks,[5,32] the ratio of the integrated intensity of the peak for methane in large cages relative to that for small cages could still be used to obtain structural information. Using these calculations, it became evident that, at least for some positions in the hydrate, methane occupied more large cages compared to water controls, consistent with the heterogeneity of hydrate composition in the presence of PVP and H1W85281 (Figure 2b and c). With PVP samples, peaks corresponding to ethane (2884 and 2940 cm^{-1}) and propane (2870, 2878, and 2984 cm^{-1}) were much bigger at locations 2 and 3 (Figure 2b). As well, the peak at 2904 cm^{-1} (corresponding to methane in large cages) was as large as the peak at 2914 cm^{-1} (methane peak corresponding to small cages). Similarly, in the presence of H1W85281, the contribution from ethane and propane was greater in some crystals and, also, methane was seen to occupy more large cages at some locations. Again, these results strongly indicate that hydrate formed in the presence of PVP and H1W85281 was not homogeneous in composition.

In striking contrast to the observations made with PVP and H1W85281, hydrate spectra obtained from samples formed in the presence of AFP-III resembled those obtained from hydrate formed without KHIs. Both water and AFP-III spectra showed within-sample consistency and little evidence of structural heterogeneity (Figure 2a and d). Significantly, evidence for the inhomogeneous nature of hydrate formed in the presence of PVP and H1W85281 has been previously observed in DSC[27] and gas uptake experiments,[28] but it has not been observed for hydrates formed in the presence of biological inhibitors .

C. NMR Spectroscopy. Hydrate composition revealed by Raman analysis was further characterized by ^{13}C magic angle spinning (MAS) NMR spectra. In hydrates formed in water controls, five peaks were observed (Figure 3a). All the peaks were associated with mixed gas sII hydrates, including peaks at −4.36 and −8.25 ppm representing methane in small and large sII

dx.doi.org/10.1021/ef200814z |*Energy Fuels* 2011, 25, 4398–4404

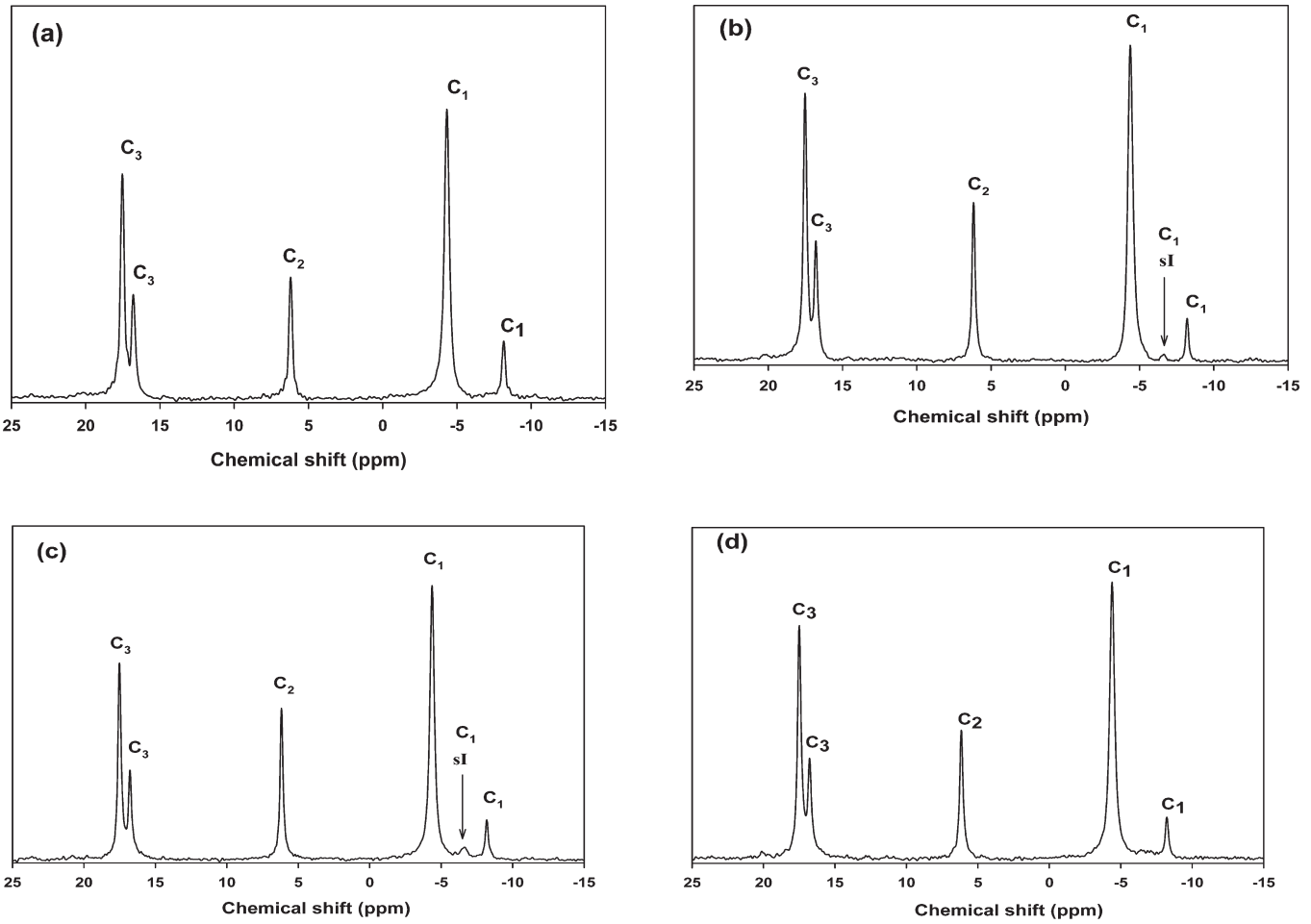

Figure 3. ^{13}C NMR spectrum of methane/ethane/propane hydrate formed with (a) no additives (control experiments), (b) PVP, (c) H1W85281, and (d) AFP-III.

Table 2. Hydrate Phase Composition of the Hydrate Synthesized in the Presence of Water or Various Inhibitors

inhibitor	methane (%)	ethane (%)	propane (%)
none	62.8	13.3	23.9
PVP	58.5	17.9	23.6
H1W85281	57.4	17.1	25.5
AFP	60.0	15.2	24.8

cages, the 6.15 ppm peak representing ethane in sII large cages, and peaks at 16.81 (methylene carbons) and 17.52 ppm (methyl carbons) representing propane in the sII large cages.[10−12] These same predominant peaks were identified in the ^{13}C MAS NMR spectra of hydrate samples synthesized in the presence of KHIs, except that an additional small peak at −6.61 ppm was observed in the PVP and H1W85281 samples (Figure 3b and c; see arrow). This peak represented methane in sI cages. Thus, NMR analysis of these samples supports the sI hydrate evidence derived from the gas phase analysis, PXRD patterns, and Raman spectroscopy (Table 1; Figures 1 and 2). It must be noted that, in contrast, no distinct peak at −6.61 was identified in the NMR spectrum obtained from the AFP-containing hydrates (Figure 3d), again consistent with the more homogeneous Raman spectral analysis in such samples.

The average hydrate gas composition was also calculated from the ^{13}C NMR data (Table 2). Although the propane concentration was approximately the same in all samples, there was less enclathrated methane found in the presence of any of the inhibitors compared to controls, consistent with the gas phase analysis. Interestingly, although enclathrated ethane increased in the presence of KHIs, the increase over hydrates formed without inhibitors was doubled in samples containing the two chemical inhibitors (∼30% increase) compared to those with AFP-III (∼15% increase).

To more fully describe the distinct differences in guest composition, the ^{13}C NMR data coupled with a statistical thermodynamic model[33,34] was used to calculate cage occupancies of the mixed gas hydrates.[9,10,12,24] These cage occupancies were then used to calculate the average hydration number, defined as the number of host molecules per guest molecule. As seen in the gas composition analysis, propane occupancy of large cages was similar in all experiments (Table 3). Small cages were 93−97% occupied by methane, but in the presence of any of the inhibitors, the ratio of small to large cage occupancy by methane changed from 4.1 to 5.2−5.7. This was mainly due to the ∼25% reduction of methane in large cages in the presence of any of the inhibitors (Table 3), consistent with hydrate gas composition (Table 2). Large cages were almost fully occupied (97−99%) by methane, ethane, or propane when formed in the

Table 3. Cage Occupancy Values Obtained with ^{13}C MAS NMR Spectra in the Presence of Inhibitors

	methane		ethane	propane		
inhibitor	small cage occupancy, θ_S	large cage occupancy, θ_L	large cage occupancy, θ_L	large cage occupancy, θ_L	total large cage occupancy	hydration number
none	0.96	0.23	0.26	0.48	0.97	5.88
PVP	0.95	0.18	0.35	0.46	0.99	5.88
H1W85281	0.93	0.17	0.33	0.49	0.99	5.96
AFP	0.97	0.17	0.28	0.47	0.92	5.94

presence of water or the chemical KHIs (PVP and H1W85281). However, the overall occupancy of large cages was somewhat lower (92%) in the AFP-containing hydrates, reflecting the smaller increase in enclathrated ethane seen in the gas occupancy and composition analysis (Tables 2 and 3). Nevertheless, in the presence of any of the KHIs, substantially more ethane occupied large cages than methane, likely as a result of the preferential enclathration of the heavier hydrocarbon. When this occurs, the methane concentration in the gas phase rises, leading to an increase in the equilibrium pressure, and that, in turn, reduces the driving force for hydrate formation. Thus, it is to be expected that all of the studied KHIs reduced hydrate growth, which they do.[26−28] It should also be noted that there was little change in the average hydration number, but even the small variations were likely due to the observed compositional changes.

Preferential enclathration of individual gases in mixed gas systems has been previously reported.[2,12] However, here, we show that, in the presence of chemical KHIs, the heavier gas, ethane, appeared to encage more readily than when a hydrate was formed in the absence of inhibitors (Tables 2 and 3). The result of reducing the partial pressure of these components and the consequent increase in methane concentration in the vapor phase (Table 1) could lead to the formation of pure methane sI hydrate or methane−ethane sI hydrate, as was detected using a variety of techniques. We suspect that it was methane−ethane sI hydrate that was formed because the ethane composition increased substantially in the chemical KHI experiments, which showed strong support for sI hydrate formation.

In the presence of AFP-III, however, significantly less ethane was enclathrated (Table 3), and the methane concentration in the vapor phase was only modestly increased. Therefore, there would be a considerable reduction in the driving force for sI hydrate. Indeed, in contrast to the chemical KHI data, we saw no strong evidence for sI hydrate in the presence of the biological inhibitor. The striking decrease in the overall large cage occupancy with the AFP-III samples is curious, and we speculate that protein groups, such as methyl residues, could occupy a gas position in the hydrate, anchoring the inhibitor to the crystal and thus reducing the overall number of ethane guests. The adsorption of AFPs to model hydrates has been visually demonstrated.[35] These biological inhibitors then likely inhibit gas hydrate formation by an absorption/inhibition mechanism, as has been previously suggested.[18,19] As well, because fewer larger cages are fully occupied, this may explain the quicker dissociation of hydrates formed in the presence of AFPs than with chemical KHIs.[28] In support of this argument, it is well-known that when the fractional occupancy of cages is increased, hydrates are more stable as a result of the lower chemical potential of water.[36] Chemical KHIs may inhibit gas hydrates by increasing the heterogeneity of the crystals, resulting in not only a longer induction time but also a longer decomposition time, which we and others have previously observed.[37] Taken together, these experiments unequivocally demonstrate that the chemical and biological KHIs are distinct in their inhibition mechanisms and thus will likely find practical utility under different conditions.

IV. CONCLUSIONS

The formation of hydrates from a synthetic natural gas mixture consisting of methane, ethane, and propane was perturbed by two different classes of KHIs: the commercial, chemical inhibitors PVP and H1W85281 and the biological inhibitor AFP-III. Gas hydrates made in a batch reactor were monitored with gas chromatography as the synthesis progressed and extensively analyzed with a variety of molecular techniques after formation. As predicted and as demonstrated by NMR spectroscopy, sII hydrates predominated, but a peak representing sI hydrate was also seen in the presence of the chemical inhibitors. A sI peak was difficult to detect in AFP-III studies. Raman spectroscopy confirmed that hydrates in the chemical KHI experiments were heterogeneous in contrast to the seemingly homogeneous hydrates formed in water controls or AFP-III experiments. As has been previously observed with gas mixtures, the gas phase methane concentration increased during synthesis, but this fractionation effect, confirmed by NMR and Raman spectroscopy, was rather more dominant in the presence of the chemical KHIs. Large hydrate cages formed in the presence of all the inhibitors showed a reduction in methane. With the commercial inhibitors, these large cage methane guests appeared to be substituted by ethane, resulting in a decreased driving force for hydrate production. Concomitant with this change, we speculated that the formed sI hydrate was likely methane−ethane sI. In contrast to the near full occupancy of total (methane + ethane + propane) large cages in chemical kinetic inhibitor experiments, almost 7% of the total large cages were not filled when hydrates were formed in the presence of AFP-III, possibly supporting an adsorption−-inhibition mechanism. This is the first time mechanisms for kinetic inhibition of natural gas hydrates by two very different classes of KHIs of natural gas hydrates have been investigated. Such studies are crucial for an academic understanding of the nature of hydrate formation as well as more practical considerations of pipeline flow assurance.

AUTHOR INFORMATION

Corresponding Author

*Phone: +1 604-822-6184. Fax: +1604-822-6003. E-mail: englezos@interchange.ubc.ca.

■ ACKNOWLEDGMENT

We would like to thank the Natural Sciences and Engineering Research Council (Canada) for their support and Shell Global Solutions for their encouragement of this research. The authors also thank Dr. Rajnish Kumar for important discussion.

■ REFERENCES

(1) Sloan, E. D. Fundamental principles and applications of natural gas hydrates. *Nature* **2003**, *426* (6964), 353–359.

(2) Uchida, T.; Takeya, S.; Kamata, Y.; Ohmura, R.; Narita, H. Spectroscopic measurements on binary, ternary, and quaternary mixed-gas molecules in clathrate structures. *Ind. Eng. Chem. Res.* **2007**, *46* (14), 5080–5087.

(3) Mehta, A. P.; Sloan, E. D. Structure-H hydrate phase-equilibria of methane plus liquid−hydrocarbon mixtures. *J. Chem. Eng. Data* **1993**, *38* (4), 580–582.

(4) Lu, H. L.; Seo, Y. T.; Lee, J. W.; Moudrakovski, I.; Ripmeester, J. A.; Chapman, N. R.; Coffin, R. B.; Gardner, G.; Pohlman, J. Complex gas hydrate from the Cascadia margin. *Nature* **2007**, *445* (7125), 303–306.

(5) Subramanian, S.; Kini, R. A.; Dec, S. F.; Sloan, E. D. Evidence of structure II hydrate formation from methane plus ethane mixtures. *Chem. Eng. Sci.* **2000**, *55* (11), 1981–1999.

(6) Ballard, A. L.; Sloan, E. D. Optimizing thermodynamic parameters to match methane and ethane structural transition in natural gas hydrate equilibria. *Ann. N. Y. Acad. Sci.* **2000**, *912*, 702–712.

(7) Uchida, T.; Moriwaki, M.; Takeya, S.; Ikeda, I. Y.; Ohmura, R.; Nagao, J.; Minagawa, H.; Ebinuma, T.; Narita, H.; Gohara, K.; Mae, S. Two-step formation of methane−propane mixed gas hydrates in a batch-type reactor. *AIChE J.* **2004**, *50* (2), 518–523.

(8) Schicks, J. M.; Naumann, R.; Erzinger, J.; Hester, K. C.; Koh, C. A.; Sloan, E. D. Phase transitions in mixed gas hydrates: Experimental observations versus calculated data. *J. Phys. Chem. B* **2006**, *110* (23), 11468–11474.

(9) Kida, M.; Hachikubo, A.; Sakagami, H.; Minami, H.; Krylov, A.; Yamashita, S.; Takahashi, N.; Shoji, H.; Khlystov, O.; Poort, J.; Narita, H. Natural gas hydrates with locally different cage occupancies and hydration numbers in Lake Baikal. *Geochem., Geophys., Geosyst.* **2009**, *10*, Q05003.

(10) Kida, M.; Sakagami, H.; Takahashi, N.; Hachikubo, A.; Shoji, H.; Kamata, Y.; Ebinuma, T.; Narita, H.; Takeya, S. Estimation of gas composition and cage occupancies in $CH_4-C_2H_6$ hydrates by CP-MAS C-13 NMR technique. *J. Jpn. Pet. Inst.* **2007**, *50* (3), 132–138.

(11) Subramanian, S. Measurements of clathrate hydrates containing methane and ethane using Raman spectroscopy. Ph.D. Thesis, Colorado School of Mines, Golden, CO, 2000.

(12) Kumar, R.; Linga, P.; Moudrakovski, I.; Ripmeester, J. A.; Englezos, P. Structure and kinetics of gas hydrates from methane/ethane/propane mixtures relevant to the design of natural gas hydrate storage and transport facilities. *AIChE J.* **2008**, *54* (8), 2132–2144.

(13) Seo, Y.; Kang, S. P.; Jang, W. Structure and composition analysis of natural gas hydrates: C-13 NMR spectroscopic and gas uptake measurements of mixed gas hydrates. *J. Phys. Chem. A* **2009**, *113* (35), 9641–9649.

(14) Susilo, R.; Lee, J. D.; Englezos, P. Liquid−liquid equilibrium data of water with neohexane, methylcyclohexane, *tert*-butyl methyl ether, *n*-heptane and vapor−liquid−liquid equilibrium with methane. *Fluid Phase Equilib.* **2005**, *231* (1), 20–26.

(15) Kelland, M. A. History of the development of low dosage hydrate inhibitors. *Energy Fuels* **2006**, *20* (3), 825–847.

(16) Koh, C. A. Towards a fundamental understanding of natural gas hydrates. *Chem. Soc. Rev.* **2002**, *31* (3), 157–167.

(17) Walker, V. K.; Zeng, H.; Gordienko, R.; Kuiper, M. J.; Huva, E. I.; Ripmeester, J. A. The mysteries of memory effect and its elimination with antifreeze proteins. In *Proceedings of 6th International Conference on Gas Hydrates*, Vancouver, July 2008.

(18) Zeng, H.; Moudrakovski, I. L.; Ripmeester, J. A.; Walker, V. K. Effect of antifreeze protein on nucleation, growth, and memory of gas hydrates. *AIChE J.* **2006**, *52* (9), 3304–3309.

(19) Zeng, H.; Wilson, L. D.; Walker, V. K.; Ripmeester, J. A. The inhibition of tetrahydrofuran clathrate−hydrate formation with antifreeze protein. *Can. J. Phys.* **2003**, *81* (1−2), 17–24.

(20) Sloan, E. D.; Koh, C. A. *Clathrate Hydrates of Natural Gases*, 3rd ed.; CRC Press Taylor & Francis Group: New York, 2008.

(21) Tulk, C. A.; Ripmeester, J. A.; Klug, D. D. The application of Raman spectroscopy to the study of gas hydrates. *Ann. N. Y. Acad. Sci.* **2000**, *912*, 859–872.

(22) Sum, A. K.; Burruss, R. C.; Sloan, E. D. Measurement of clathrate hydrates via Raman spectroscopy. *J. Phys. Chem. B* **1997**, *101* (38), 7371–7377.

(23) Ripmeester, J.; Ratcliffe, C. On the contributions of NMR spectroscopy to clathrate science. *J. Struct. Chem.* **1999**, *40*, 654.

(24) Ripmeester, J. A.; Ratcliffe, C. I. Low-temperature cross polarization/magic angle spinning ^{13}C NMR of solid CH_4 hydrates: structure, cage occupancy, and hydrate numnber. *J. Phys. Chem.* **1988**, *92* (2), 337.

(25) Ohno, H.; Strobel, T. A.; Dec, S. F.; Sloan, E. D.; Koh, C. A. Raman studies of methane−ethane hydrate metastability. *J. Phys. Chem. A* **2009**, *113* (9), 1711–1716.

(26) Ohno, H.; Susilo, R.; Gordienko, R.; Ripmeester, J.; Walker, V. K. Interaction of antifreeze proteins with hydrocarbon hydrates. *Chem.—Eur. J.* **2010**, *16* (34), 10409–10417.

(27) Daraboina, N.; Ripmeester, J. A.; Walker, V. K.; Englezos, P. Natural gas hydrate formation and decomposition in the presence of kinetic inhibitors. 1. High pressure calorimetry. *Energy Fuels* **2011**, DOI: 10.1021/ef200812m.

(28) Daraboina, N.; Ripmeester, J. A.; Walker, V. K.; Englezos, P. Natural gas hydrate formation and decomposition in the presence of kinetic inhibitors. 2. Stirred reactor experiments. *Energy Fuels* **2011**, DOI: 10.1021/ef200813v.

(29) Linga, P.; Kumar, R.; Englezos, P. Gas hydrate formation from hydrogen/carbon dioxide and nitrogen/carbon dioxide gas mixtures. *Chem. Eng. Sci.* **2007**, *62* (16), 4268–4276.

(30) Linga, P.; Kumar, R.; Englezos, P. The clathrate hydrate process for post and pre-combustion capture of carbon dioxide. *J. Hazard. Mater.* **2007**, *149* (3), 625–629.

(31) Sloan, E. D., Jr. *Clathrate Hydrates of Natural Gases*, 2nd ed., Revised and Expanded; Marcel Dekker: New York, 1998; p 754.

(32) Subramanian, S.; Sloan, E. D. Trends in vibrational frequencies of guests trapped in clathrate hydrate cages. *J. Phys. Chem. B* **2002**, *106* (17), 4348–4355.

(33) van der Waals, J. H.; Platteeuw, J. C. Validity of Clapeyron's equation for phase equilibria involving clathrates. *Nature* **1959**, *183* (4659), 462.

(34) van der Waals, J. H.; Platteeuw, J. C. Clathrate Solutions. In *Advances in Chemistry*; InterScience: New York, 1959; Vol. II, pp 1−58.

(35) Gordienko, R.; Ohno, H.; Singh, V. K.; Jia, Z. C.; Ripmeester, J. A.; Walker, V. K. Towards a green hydrate inhibitor: imaging antifreeze proteins on clathrates. *PloS ONE* **2010**, *5* (2), Gordienko.

(36) Dec, S. F.; Bowler, K. E.; Stadterman, L. L.; Koh, C. A.; Sloan, E. D. NMR study of methane plus ethane structure I hydrate decomposition. *J. Phys. Chem. A* **2007**, *111* (20), 4297–4303.

(37) Makogon, Y. F.; Holditch, S. A. Lab work clarifies gas hydrate formation, dissociation. *Oil Gas J.* **2001**, *99* (6), 47.